Saudi Pharmaceutical Journal 29 (2021) 1449–1457

Contents lists available at ScienceDirect

Saudi Pharmaceutical Journal

journal homepage: www.sciencedirect.com

Original article

Design and Characterization of Atorvastatin Dry Powder Formulation as a potential Lung Cancer Treatment

Alaa S. Tulbah [a,*], Amr Gamal [b]

[a] Department of Pharmaceutics, College of Pharmacy, Umm Al-Qura University, Makkah, Saudi Arabia
[b] Department of Pharmaceutics and Industrial Pharmacy, Faculty of Pharmacy, Beni-Suef University, Beni-Suef, Egypt

ARTICLE INFO

Article history:
Received 29 August 2021
Accepted 5 November 2021
Available online 11 November 2021

Keywords:
Lung cancer
Dry Powder Inhaler
Mannitol
Aerodynamic
Cytotoxicity

ABSTRACT

Lung cancer is the leading cause of cancer death. Many studies have shown the beneficial effects of Atorvastatin in decreasing the mortality risk and improving survival among patients with lung cancer. This research paper focuses on improving AVT cytotoxic activity and cellular uptake by developing mannitol microcarriers as a promising drug delivery system for lung cancer treatment and, studying the impact of improving inhalation deposition on the delivery and Dry Powder formulations efficiency. The AVT loaded mannitol (AM) microparticles (AVT-AM) formulation was prepared by spray drying and characterized for its physicochemical properties and aerodynamic deposition. The results revealed that the AVT-AM formulation has good flow properties and aerosol deposition with a particle size of 3418 nm ± 26.86. The formulation was also assessed in vitro for cytotoxicity effects (proliferation, apoptosis, and cell cycle progression) on A549 human lung adenocarcinoma. Compared with free AVT, the AVT-AM formulation has significantly higher cellular uptake and anti-cancer properties by disrupting cell cycle progression via either apoptosis or cell cycle arrest in the G2/M phase. This study shows that AVT loaded mannitol microcarriers may provide a potentially effective and sustained pulmonary drug delivery for lung cancer treatment.

© 2021 The Authors. Published by Elsevier B.V. on behalf of King Saud University. This is an open access article under the CC BY-NC-ND license (http://creativecommons.org/licenses/by-nc-nd/4.0/).

1. Introduction

Lung cancer is a type of pulmonary neoplasm that causes uncontrolled cell proliferation in lung tissues (Singh & Changotra, 2019). Besides, it is currently the main cause of cancer mortality worldwide (W.-H. Lee et al., 2018; Xia, Hu, Tian, & Zeng, 2019). A major modifiable lung cancer risk factor is exposure to tobacco smoking (Mustafa et al., 2016). Atorvastatin (AVT) is an oral cholesterol-lowering agent widely used to reduce cholesterolemia and manage cardiocerebrovascular (Xia et al., 2019). Recently, many studies have shown beneficial effects of AVT on the lung cancer incidence (Khurana, Bejjanki, Caldito, & Owens, 2007; Lin, Ezer, Sigel, Mhango, & Wisnivesky, 2016; Xia et al., 2019). AVT decreases small G-protein activity, which is regularly vital in cell proliferation, angiogenesis, and tumor growth of the lung cancer. Additionally, AVT reduces the mortality risk and improves survival among patients with lung cancer. Pulmonary delivery of drugs is an ideal route for lung cancer treatment compared with oral and injection routes due to the potential reduction in systemic toxicities, increased local concentration of drugs, and avoidance of first-pass metabolism (W.-H. Lee et al., 2018; W.-H. Lee, Loo, Traini, & Young, 2021).

Dry powder inhalers (DPIs) are the most used inhalation route and have been studied for lung cancer treatment (Gamal, Saeed, Sayed, Kharshoum, & Salem, 2020; W.-H. Lee et al., 2021; Tulbah et al., 2015). DPIs are propellant-free dosage forms in which powdered therapeutic agents are inhaled into the respiratory tract. They have better stability and lack many drawbacks related to MDIs and nebulizers (Peng et al., 2016). In addition, DPIs have the advantage of dose precision in dosing and patient competence (Tulbah et al., 2015). However, DPIs produce micron-sized particulates which exhibit greater cohesiveness and adhesiveness with poor flow and entrainment properties. These formulation chal-

* Corresponding author.
E-mail addresses: astulbah@uqu.edu.sa (A.S. Tulbah), amr_g@pharm.bsu.edu.eg (A. Gamal).

Peer review under responsibility of King Saud University.

Production and hosting by Elsevier

https://doi.org/10.1016/j.jsps.2021.11.002
1319-0164/© 2021 The Authors. Published by Elsevier B.V. on behalf of King Saud University.
This is an open access article under the CC BY-NC-ND license (http://creativecommons.org/licenses/by-nc-nd/4.0/).

lenges can be resolved by blending the drug with an inert carrier such as lactose and mannitol to achieve reproducible and high pulmonary deposition (Gamal et al., 2020; Kaialy, Martin, et al., 2012a). Although lactose is a coating carrier commonly used in DPI formulations, it produces larger particles that generate poorer performance in DPI inhalation and cannot be used for compounds that interfere with the lactose's reduced sugar feature such as, peptides and budesonide.

Mannitol (AM) has several benefits over lactose because its particles seem to be slightly longer, with more surface irregularities and a smaller volume mean diameter, which enhances the inhalation efficiency and pulmonary deposition of DPIs (Gamal et al., 2020; Kaialy, Martin, et al., 2012a). In addition, mannitol also improves mucus fluidity via osmotic pressure, enhancing its clearance from the lung (Ong et al., 2014). This study focuses on improving AVT cytotoxic activity and cellular uptake by developing mannitol microcarriers as a promising drug delivery system for lung cancer treatment, as well as studying the impact of improving inhalation deposition on the delivery and efficiency of Dry Powder formulations. The in vitro characterization of the co-engineered AVT-mannitol (AVT-AM) formula was evaluated to investigate its physico-chemical properties and in vitro aerosol performance. Moreover, the formula was also assessed in vitro for cytotoxicity effects (proliferation, apoptosis, and cell cycle progression) on A549 human lung adenocarcinoma.

2. Materials and Methods

2.1. Materials

Atorvastatin calcium, Sulforhodamine-B (SRB), and mannitol were obtained from Sigma Aldrich, USA. Methanol, ethanol, and acetonitrile obtained from Thermo-Fisher, Europe. A cell line for non-small lung cancer (A549), cell culture materials, and WST kits were obtained from Corning, USA.

2.2. Preparation of atorvastatin mannitol microparticles

The spray drying methodwas applied to prepare the AVT-AM formula (Ong et al., 2014). Briefly, water was used for mannitol and atorvastatin dissolving to prepare a solution of 99.8% w/w mannitol and 0.2% w/w atorvastatin. A spray dryer (Flawil, Switzerland) was utilized to generate AM powders with a 20 mg/mL feed concentration, a 4 mL/min feed rate, a 47.6 $m^3\ h^{-1}$ suction rate, a 600 kPa atomizing pressure, and a 150 °C inlet temperature.

2.3. In vitro evaluation of atorvastatin mannitol microparticles

2.3.1. HPLC quantification of atorvastatin

The AVT quantification was carried out by the HPLC method (Stanisz & Kania, 2006). The quantification was obtained through analytical column C-18 with 250 × 4.6 mm using a mobile phase composed of buffer solution (pH 3) of orthophosphoric acid and acetonitrile at a ratio of 70:30 v/v. The AVT detection was processed at a maximum wavelength of 254 nm and with a 1 mL/min mobile phase flow and an injection volume of 20 μL. The drug retention time, flow rate, and run time were 4.372 min, 1 mL/min, and 6 min, respectively. Also, the mode of elution was isocratic.

2.3.2. Evaluation of percentage recovery and encapsulation efficiency

The measurement of % recovery of AVT-AM formula was obtained by dividing the spray-dried AVT-AM formula weight and the weight of AVT and mannitol, separately, as follows (Dixit, Kini, & Kulkarni, 2010):

$$\%\ \text{Recovery} = \frac{\text{The spray} - \text{dried powder weight}}{\text{The initial powders weight before spray drying}} \times 100 \quad (1)$$

The encapsulation efficiency of the produced microparticles was measured by accurately weighing 10 mg of the powder and dissolving it in the mobile phase. The drug concentration in the produced solution was defined using the previously described method (Dixit et al., 2010):

$$\%\ \text{Encapsulation efficiency} = \frac{\text{The AVT content of spray} - \text{dried powder}}{\text{The initial AVTcontent}} \times 100 \quad (2)$$

2.3.3. Particle size and polydispersity index determination

The AVT-AM formula was blended with water (distilled), and the average size and distribution of AVT-AM formulae were measured by Mastersizer (Malvern, UK) (Tulbah et al., 2015). Around 5 mg of powder was performed in triplicates by applying the dry dispersion technique.

2.3.4. Measurement of micromeritics properties

A microscopic method using a calibrated ocular micrometer measured the micromeritics AVT-AM formula powders properties (Dixit et al., 2010). A Pycnometer was used to measure the apparent particle densities of microparticles. Carr's index was used to measure the formula powders' flow properties as follows:

$$\text{CI} = \frac{\text{TD} - \text{BD}}{\text{TD}} \times 100 \quad (3)$$

where, BD is the bulk density obtained by dividing the AVT-AM formula powder mass by its bulk volume. TD is the tapped density measured by dividing the tapped AVT-AM formula powder mass by its tapped volume.

2.3.5. Measurement of morphology

Transmission electron microscopy was used to measure the morphology of the AVT-AM formula using TEM, JEM- 2100, Plus Electron Microscope (JEOL, Japan) (Gamal et al., 2020). The powder samples (0.1 mg/mL) were combined in a phosphate buffer before being sonicated for 1 minute in an ice bath. The diluted solution (one drop) was applied to a 200- carbon-coated mesh TEM grid and left to dry. At room temperature, 4 percent osmium of tetroxide was added to the grids to increase contrast and left to dry. Then, immediately photographed at 120 kV with TEM. TEM photographs were taken at different magnifications.

Scanning electron microscope (Zeiss Sigma 500 VP analytical field emission (FE)-SEM, Carl Zeiss, Germany) was selected for SEM image and powder surface morphology (Tulbah et al., 2015). The powder sample was mounted on aluminium stubs and then gold at 20 nm was used to coat the sample. SEM images were carried at different magnifications.

2.3.6. Thermal properties analysis

Differential scanning calorimetric (DSC-60A, Shimadzu, Japan) was applied to detect the thermal state, compatibility, and crystallinity of AVT-AM formula components (Dixit et al., 2010). In an aluminum pan, around a small amount of mannitol, AVT-AM microparticles, and free AVT powder were sealed, and the recorded heat flow was at 10 °C/min under nitrogen gas; at 10 mL/min of flow; and from 25 °C to 300 °C with the heating scan. Data were normalized for initial mass.

2.3.7. Fourier transform infrared spectroscopy (FTIR)

The AVT presence inside mannitol microparticles was confirmed using FTIR (FTIR-8400s, Shimadzu, Kyoto, Japan) in the mid-infra range of 400 to 4000 cm^{-1} wavenumbers (Dixit et al., 2010).

2.3.8. Aerodynamic characterization

The Appendix XII F of the British Pharmacopeia (2005) described the basic methodology of aerodynamic characterization (Salem, Abdelrahim, Eid, & Sharaf, 2011). In brief, 250 mg of AVT-AM formula was loaded into five size-3 capsules before being employed inside an Aerolizer DPI (Foradil™ device). The Andersen MKII Cascade Impactor (ACI) was used to determine their aerodynamic characteristics. Stages -0 and -1 were assembled instead of stages 0 and 7 (Saeed, Salem, Rabea, & Abdelrahim, 2019). All ACI portions were washed in the mobile phase and the plates were sprayed with silicone fluid. All ACI portions were assembled and sealed with parafilm M laboratory film. Each capsule was employed inside DPI and released into the ACI device under a 60 L/min flow rate for 4 seconds to allow inhalation of 4 L of air (Pharmacopeia, 2015). The drug amount deposited on each stage was rinsed with the mobile phase and was determined by a previously validated HPLC method. For each powder, five separate determinations were made (n = 5). The total emitted dose (TED), the mass median aerodynamic diameter (MMAD, μm), fine particle dose (FPD, μg), and fine particle fraction (FPF %) were measured using impactor data evaluation CITDAS software (Copley Scientific, UK).

2.4. In vitro bio-characterization of atorvastatin mannitol microparticles

2.4.1. Cell culture

A549 ($5x10^3$ cells/well) human lung adenocarcinoma cells were preserved in DMEM medium supplemented with 100 mg/mL of penicillin/streptomycin, higher glucose levels of 4500 mg/L and 10% of heat-inactivated fetal bovine serum. Cells were cultured in a humidified incubator at 37 °C with 5% CO_2 until confluency was reached. ATCC recommended guidelines were followed for each cell passage step (Marin et al., 2013).

2.4.2. Cytotoxicity assay

The sulphorhodamine B (SRB) assay allowed researchers to quickly and accurately measure drug cytotoxicity in cell culture. The cytotoxicity of the AVT-AM formula and free AVT solution was evaluated using A549 human lung adenocarcinoma cells, as previously described (Allam et al., 2018). Briefly, 96-well plates were filled with A549 cell suspension (100 μL, $5x10^3$ cells) and cultured for 24 hours in complete media. The AVT-AM formula and AVT solution (0.3–1000 μg/mL) were incubated in the cells and, after 72 h of exposure, trichloroacetic acid (TCA, 150 μL, 10%) was added and incubated for 1 hour at 4 °C to fix the cells. After TCA removal, the cells were washed and incubated with distilled water and SRB solution (70 μL, 0.4% w/v), respectively, for 10 min at 25 °C. Acetic acid (1%) was used to wash the plates 3 times. The protein-bound SRB stain was used to dissolve it in TRIS (150 μL, 10 mM). The Omega microplate reader (BMG LABTECH®-FLUOstar, Ortenberg, Germany) was used to measure the absorbance at 540 nm. As previously described by Tulbah et al, the viable cell percentage relative to the untreated control was used to verify cell viability (Tulbah et al., 2019). IC_{50} of the drug concentration was defined as causing a 50 % reduction in cell viability. Plotting cell viability percentage versus the concentrations (μg/mL) was used to calculate the IC_{50} values. The IC_{50} plot illustrates the nonlinear fit of "Transform" and "Normalize" of the obtained data. The GraphPad Prism 9 software was utilized to measure the data value as the "best fit value."

2.4.3. Cellular uptake assay

After defining the AVT proper concentration safe for the A549 cell line, cellular uptake of the formula was studied. The cellular uptake of the AVT-AM formula and free AVT solution was running on the cells. On the first day, a T25 flask was used to seed the cells at 0.7×10^6 and incubated at 37 °C and 5% CO_2. The media were removed on the second day, replaced with 10 g/mL of both treatments and incubated at different time points of 6 and 24 h at 37 °C and 5% CO_2 to assist the cellular uptake. At each time point, the cells were lysed as described by Guntner et al. (Guntner, Doppler, Wechselberger, Bernhard, & Buchberger, 2020). To achieve this, the cells were washed 2 times with a phosphate buffer solution. Consequently, the cells were centrifuged after trypsinization. Before, ultrasonic treatment for 2 min, ethanol, acetonitrile, and water (2:2:1) were used to lyse the collected cell pellets. Then, the supernatant was centrifuged for 10 min at 13,000 rpm and the drug amount was determined by a previously HPLC method. Finally, the cellular uptake calculation was standardized with total proteins and expressed as ug/total protein (ug) (W.-H. Lee et al., 2016).

2.4.4. Apoptosis assay

The Apoptosis detection kit (Annexin V-FITC, Abcam, UK) coupled with two fluorescent channels flow-cytometry was used to evaluate the impact of the AVT-AM formula on apoptosis, necrosis cell populations, and programmed cell death (Fekry et al., 2019). Briefly, 10 μg/mL of AVT-AM formula was used to treat the cells for one day, then trypsinized and washed 2x with ice-cold PBS (pH 7.4). The cells were dyed using Annexin V-FITC/PI solution (0.5 mL, 30 min, 25 °C) and injected via flow-cytometer (ACEA, USA). The PI (λex/em 535/617 nm) and FITC (λex/em 488/530 nm) fluorescent signals were analysed by FL1 and FL2 signal detectors for each sample, respectively, and quantified by ACEA NovoExpress™ software.

2.4.5. Autophagy assay

Acridine orange lysosomal dye with flow-cytometric was used to evaluate the method of autophagic cell death by the AVT-AM formula (Fekry et al., 2019). Briefly, 10 μg/mL of AVT-AM formula was used to treat the cells for one day, then trypsinized and washed twice with ice-cold PBS (pH 7.4). Next, the cells were stained with acridine orange solution (10 μM, 30 min, 37 °C) and injected via flow-cytometer (ACEA, USA). For each sample, acridine orange fluorescent signals were analysed using FL1 (λex/em 488/530 nm) signal detector and quantified using ACEA NovoExpress™ software.

2.4.6. Analysis of cell cycle distribution

Flow-cytometry analysis was employed to evaluate the effect of the AVT-AM formula on cell cycle distribution (Fekry et al., 2019). Briefly, 10 μg/mL of AVT-AM formula was used to treat the cells for one day, then trypsinized and washed twice with ice-cold PBS (pH 7.4). Next, the cells were held in PBS (1 mL) containing RNAase A (50 μg/mL) and propidium iodide (PI, 10 μg/mL) for 20 min and at 37 °C and injected via flow-cytometer (ACEA, USA). The DNA content was analysed for each sample using FL2 (λex/em 535/617 nm) signal detector and cell cycle distribution quantified using ACEA NovoExpress™ software.

2.5. Statistical analysis

Triple different determinants of each data are expressed as "mean ± standard deviation (S.D.)". IBM-SPSS Statistics (version

22, USA, P 0.05) was used to run one-way ANOVA and unpaired two-tailed t-tests.

3. Results and Discussion

3.1. AM formula powder preparation and in vitro characterization

Powder formulation properties are one of the most important factors of DPI performance (Kaialy, Ticehurst, & Nokhodchi, 2012b; Young, Traini, Coates, & Chan, 2007). The carrier is blended with a drug to produce a high degree of drug aerosolization and enhance DPI performance. Mannitol was used as an alternative sugar for dry powder inhalations (Steckel & Bolzen, 2004). Despite this, their chemical characteristics differ significantly, with lactose being a reducing sugar and mannitol lacking this ability due to the carbonyl group absence, which is present in lactose (Ferdynand & Nokhodchi, 2020; Gamal et al., 2020). Mannitol is highly wettable and can decrease disintegration time, assisting the drug release (Steckel & Bolzen, 2004). Mannitol increases protection against moisture in formulations, improving their chemical/physical stability (Abd-Elbary, El-Laithy, & Tadros, 2008). The concentration of mannitol and AVT in the feed solution was chosen based on data collected from the literature review to produce mannitol microparticles with suitable particle size, flow properties, and % EE (Ong et al., 2014; Tee, Marriott, Zeng, & Martin, 2000). Successfully, the AVT-AM formula was prepared using the spray drying method with relative concentrations of 99.8% w/w mannitol and 0.2% w/w AVT in the feed solution.

The HPLC method was used to quantify AVT with linearity between 15.625 and 250 μg/mL and a determination coefficient (R^2) of 0.99. The % EE was examined to assess the drug content of the developed formula. The % EE was found to be 98 ± 1.87 %. The powders recovery can be clarified well in terms of flow properties because poor flowable nanoparticles typically have low recovery (Plumley et al., 2009). The recovery % was found to be 80.62 ± 2.13%. Because of the microparticles' improved wet ability and an AVT existence amorphous form in microparticles, spray drying has a high potential to enhance the solubility of weakly aqueous drugs like AVT (Dixit et al., 2010). Increasing the AVT solubility resulted in increasing drug loading and better entrapping AVTefficiency.

The particle size determination results revealed that spray-dried AVT-AM microparticles were small and homogeneous in size, which contributed to the improvement of the generated microparticles' physicochemical attributes. The results revealed a low polydispersity index of 0.367 ± 0.07, indicating a homogenous microparticles distribution and a particle size of 3418 ± 26.86 nm. These results were obtained because mannitol produces microparticles with an elongated shape. These findings matched those of the Abd-Elbary et al. study (Abd-Elbary et al., 2008), suggesting the AVT-AM formula was suitable for inhalation applications.

The AVT-AM formula flow properties were important for homogenous filling of the DPI and improvement of accurate dose delivery (Gamal et al., 2020). Carr's index (% CI) was applied to verify the flow properties of powders. The % CI outcomes indicated that the AVT-AM formula has good flow properties. The large size of vesicles resulted in higher flow properties by reducing the surface area of particles and reducing the tendency for aggregation (Gupta et al., 2000; Vanbever et al., 1999).

Fig. 1 shows TEM (A) and SEM (B) images of the surface morphology of AVT-AM microparticles. The TEM and SEM results revealed that spray-dried microparticles were spherical in shape and appeared as black/white dots, indicating that they were more stable and less prone to caking.

The crystalline properties and thermal behaviour of mannitol, AVT-AM microparticles, and the free AVT are shown in Fig. 2. The DSC analysis revealed that a pure mannitol sample melted at 163.51 °C with an enthalpy of 312.10 J/g, AVT-AM formula had a melting endotherm of 163.14 °C and a lowered enthalpy of 307.45 J/g and AVT had a melting endotherm of 169.34 °C with an enthalpy of 7.02 J/g. This indicates that there was decreased crystallinity because AVT was incorporated into the microparticles structure as an amorphous form. The drug crystalline behaviour results are in a good correlation with a prior study (Bayón & Rojas, 2019). Hence, the micronized AVT-AM formula did not influence the particle physical characteristics, apart from its size.

The infrared spectra of mannitol, AVT-AM, and free AVT are shown in Fig. 3. Mannitol, AVT-AM, and free AVT all displayed a similar peak in the infrared spectrum. The free AVT showed that the aromatic out-of-plane curve was at the 690.58 cm^{-1} band, C—N stretching was at the 1309.99 cm^{-1} band, C═O groups of amid stretching were at the 1647.69 cm^{-1} band, N—H stretching was at the 3354.31 cm^{-1} band, and OH stretching was at the 3661.43 cm^{-1} and 3228.73 cm^{-1} bands. A similar result appeared

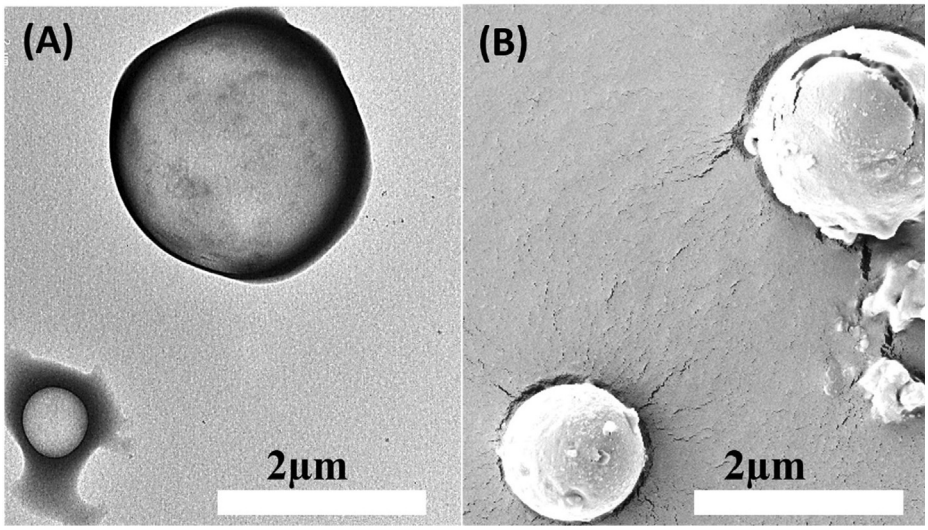

Fig. 1. The surface morphology of AVT-AM formulation using (A) TEM and (B) SEM.

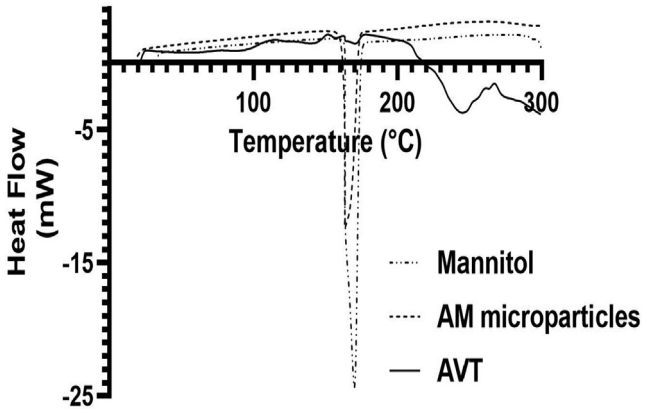

Fig. 2. The DSC of mannitol, AVT-AM formulation, and free AVT.

in another work by Shaheaeini et al. (Shahraeini et al., 2020). The mannitol FTIR was also illustrated by absorption peaks at 3274.46 cm^{-1}, 1409.35 cm^{-1}, 1012.46 cm^{-1}, and 624.90 cm^{-1}. The FTIR of AVT-AM microparticles absorption bands was observed at 3272.14 cm-^{1}, 1423.29 cm^{-1}, 1.75.34 cm^{-1}, 705.39 cm^{-1} and 621.71 cm^{-1} showing a matching spectrum in the bands stretching of combined compounds in the preparation, indicating formulation compatibility. The FTIR of the AVT-AM microparticles also declared the components' chemical interactions of the microparticles formula. This could indicate that the spray-dried microparticles of AVT have the same spectra as the pure sample, indicating that atorvastatin is present inside the microparticles.

The aerodynamic deposition of the AVT-AM formula powder was measured using the cascade impactor (Zijlstra et al., 2007). Fig. 4 demonstrates AVT-AM formula powder deposition after aerosolization on ACI stages. The results revealed that the aerodynamic deposition of AVT-AM microparticles powder showed good FPD of 113.5 ± 29.5 μg, FPF of 47.5 ± 4.6 %, and TED of 237.4 ± 29.5. MMAD was measured because the deposition site and the inhaled drug amount that deposits in the respiratory system are affected by particle size (Newman, 1985). The MMAD of the AVT-AM formula powder was 3.8 ± 0.6 μm. These results were acquired as a result of the AVT-AM powder's increased flow property, which could affect lung deposition significantly.

3.2. In vitro bio-characterization of atorvastatin mannitol microparticles

3.2.1. Cytotoxicity assay

Using the SRB assay in the A549 cell line, the cytotoxicity and cell viability of the AVT-AM formula and free AVT were examined to identify the suitable concentration range for lung delivery of the drug. As shown in Fig. 5, the AVT-AM formula and free AVT had an IC_{50} value of 10.80 μg/ml and 8.53 μg/mL, respectively. These findings suggest that the AVT-AM formula powder showed in vitro A549 cytotoxic activity, implying that mannitol could be a promising carrier for AVT that may be employed as an option for effective lung cancer treatment with fewer side effects. Additionally, the AVT-AM formula powder is safe and non-toxic on A549 cells. This finding was in alignment with Fan et al (Fan, Jiang, Wang, & Qu, 2016).

3.2.2. Cellular uptake assay

The AVT ability and extent to reach the alveolar macrophage epithelium will rely on the A549 cellular uptake of the AVT-AM formula. A549 cells are a kind of epithelial cell obtained from human lung cancer (Lieber, Smith, Szakal, Nelson-Rees, & Todaro, 1976), broadly utilized as an in vitro model of human alveolar type

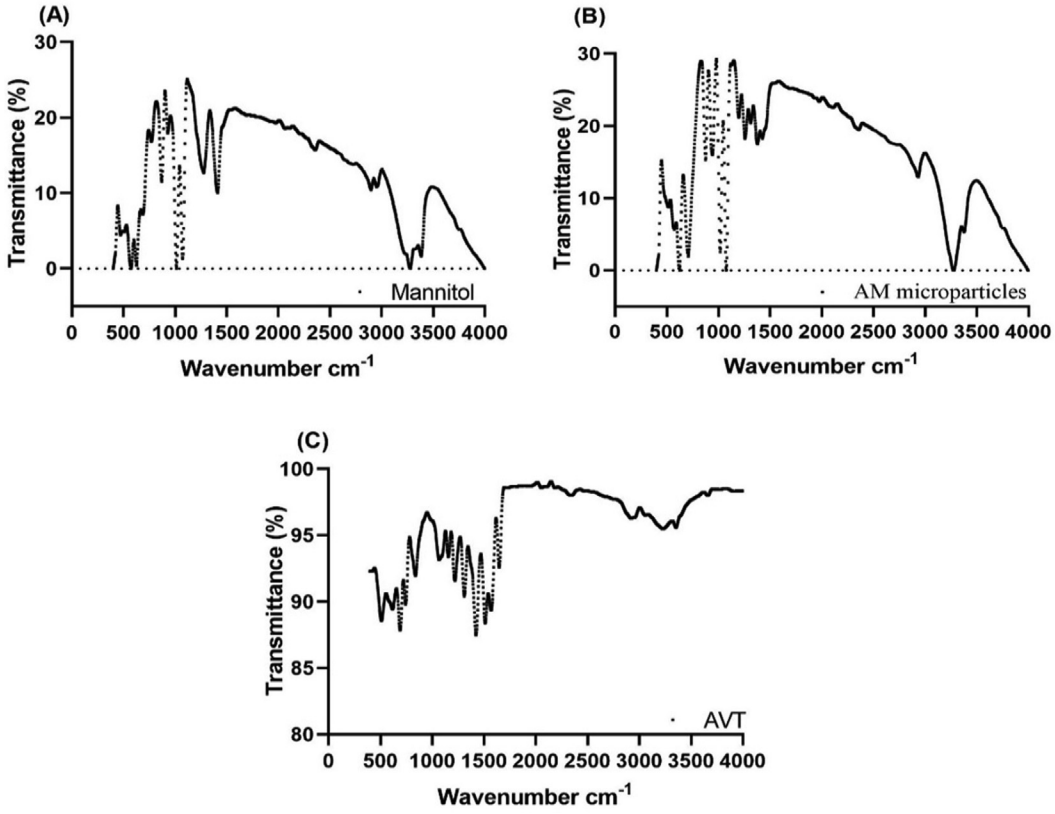

Fig. 3. The FTIR of **(A)** mannitol, **(B)** AVT-AM formulation, and **(C)** free AVT.

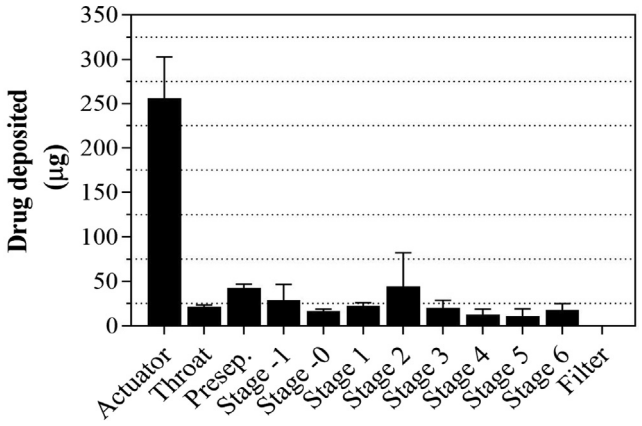

Fig. 4. In vitro drug deposition of the AVT-AM formulation by Andersen MKII Cascade Impactor (ACI) using the Foradil™ DPI device at a 60 L/min, (n = 3 ± S.D.).

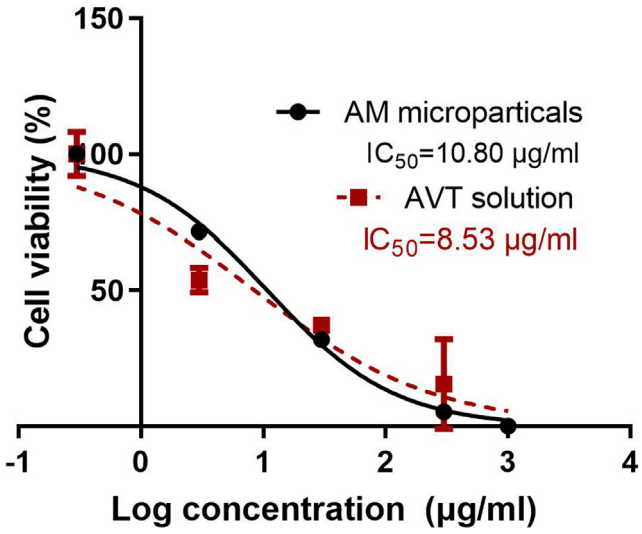

Fig. 5. The cytotoxicity of AVT-AM formulation and free AVT solution on A549 cells line model.

2 epithelial cells for biological investigations (Mörbt et al., 2011; R. C. Stearns, J. D. Paulauskis, & J. J. Godleski, 2001). The cells from confluent monolayers with morphology and function properties are alike the alveolar type 2 epithelial cells, as suggested by Foster et al. (Foster, Oster, Mayer, Avery, & Audus, 1998). The Foster group suggested that the A549 cell line as a standardized model for studying lung alveolar type II epithelium and drug metabolism (Foster et al., 1998). Phagocytosis of particles by alveolar epithelial cells was described in many research (Rebecca C Stearns, Joseph D Paulauskis, & John J Godleski, 2001).

To investigate this, the internalization of the AVT-AM formula and free AVT by the A549 cells as a time function was evaluated. Many findings have indicated that the lung is subjected to environmental particles such as air contamination, dust, and smoke. Continuous exposure to these particles stimulates alveolar macrophages to play a critical role in the intrinsic defence of the airways in lung disease patients (Dockery et al., 1993; Dockery, Schwartz, & Spengler, 1992; Pope et al., 1995; Schwartz & Dockery, 1992). Any adverse effects on the alveolar macrophage epithelium could change its morphology and phagocytic activity (Byrne, Mathie, Gregory, & Lloyd, 2015; Lohmann-Matthes, Steinmuller, & Franke-Ullmann, 1994). Therefore, the A549 cells

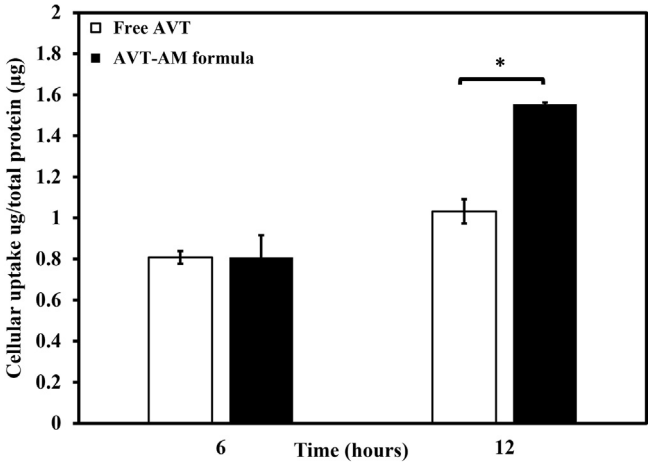

Fig. 6. Internalization of AVT after free AVT solution and AVT-AM formulation deposition on A549 cells line model. Data represent mean ± SD (n = 3). *P < 0.05 shows significant differences within the two treatments.

were treated with AVT-AM formula or free AVT at 10 µg/ml of atorvastatin concentration. As shown in Fig. 6, the cellular internalization efficacy of the AVT-AM formula and free AVT at 6 h was 0.80 µg/µg ± 0.03 and 0.81 µg/µg ± 0.05 of total protein, respectively. Interestingly, the AVT-AM formula had significantly greater cellular uptake efficacy after 24 h of incubation (1.56 µg/µg ± 0.11) compared to the free AVT (1.02 µg/µg ± 0.01). These data proved that the AVT-AM formula had significantly higher cellular uptake (P > 0.05) than the free AVT after 24 h of therapy. This improvement of the AVT-AM formula cellular uptake might be associated with electrostatic properties of the cells membrane (Mohning et al., 2018; Schneider et al., 2017). In general, the microparticles drug internalization in A549 cells could be mediated only by the phagocytosis process, whereas some free drugs surely pass through the membrane, and others are exposed to mechanisms of efflux pump (Mohning et al., 2018; Schneider et al., 2017). Thus, the increased uptake of AVT-AM formula might enhance drug delivery into A549 cells during a disease stage. A study by Fan et al. found that AVT can partially prevent the epithelial-to-mesenchymal transition of non-small cell lung cancer cells process stimulated by TGF-β1 by decreasing the sphingosine kinase 1 upregulation (Fan et al., 2016). This could reduce free drugs unwanted effects and enhance therapeutic efficacy implying that mannitol could be a promising carrier for AVT that may be employed as an option for effective lung cancer treatment with fewer side effects (Fan et al., 2016).

3.2.3. Influence of AVT-AM formulation on the cell cycle distribution, apoptosis, and autophagy of A549 cells

A DNA flow-cytometric analysis was used to investigate the atorvastatin effects on cell cycle phases, apoptosis, and autophagy of A549 human lung adenocarcinoma cells (Fig. 7). AVT-AM's antiproliferative effect can be determined using cell cycle analysis in terms of cell cycle phase specificity (G2/M-phases, S, and G0/G1) (Kuh et al., 2000). Furthermore, evaluating the cell population during apoptosis provides significant insights into potential cell-killing effects (Pucci, Kasten, & Giordano, 2000). The AVT-AM formula shows anti-cancer properties by disrupting cell cycle progression either via apoptosis or cell cycle arrest in vitro (Fan et al., 2016; J. Lee et al., 2019; Tulbah, 2020).

In general, the G0/G1 cells increased slightly from 60.16 ± 1.17% for the untreated sample to be around 60.28 ± 2.78 % when 10 µg/ml of AVT-AM was added on the cells as in Fig. 7, A. The data showed that the treatment with 10 µg/ml of AVT-AM resulted in

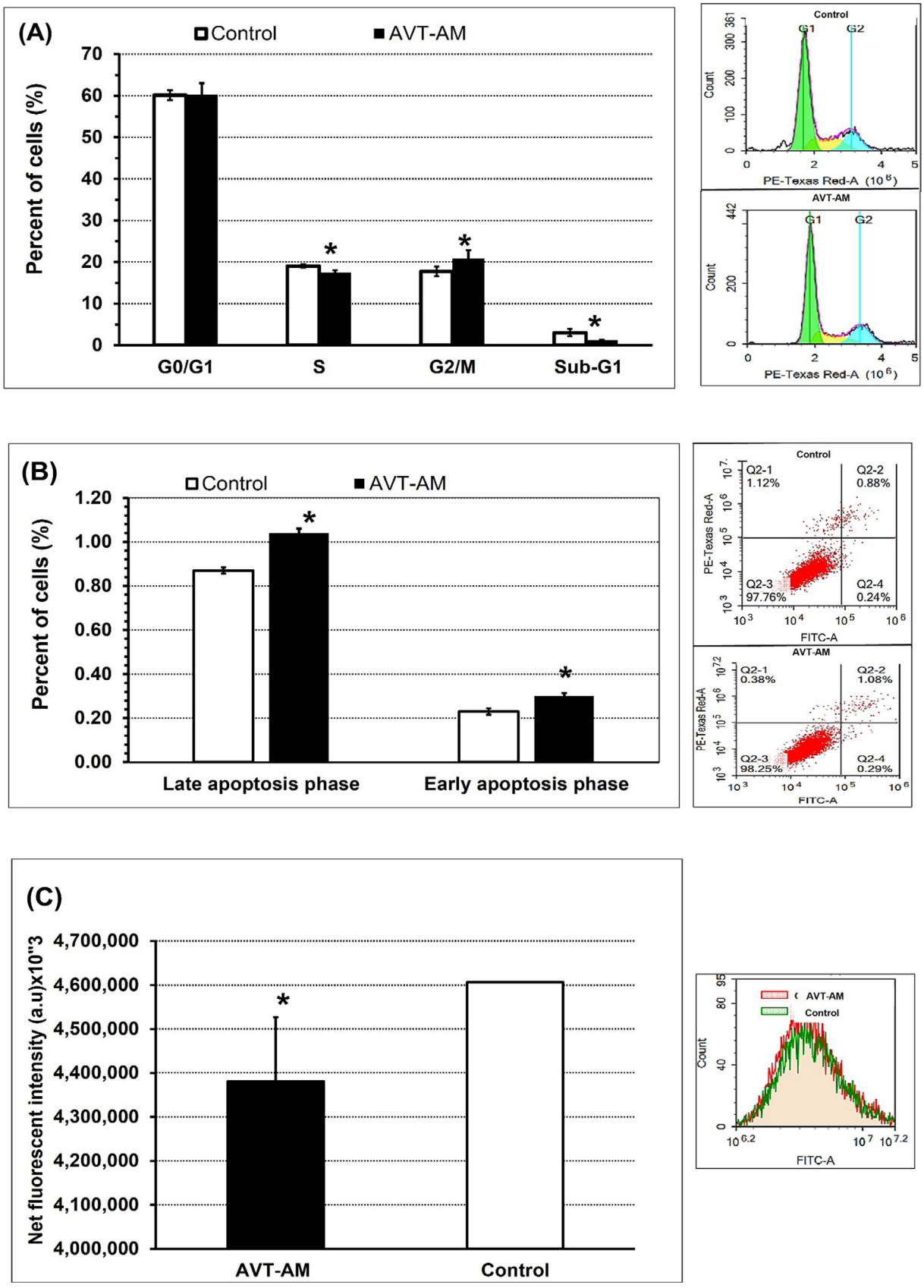

Fig. 7. The effect of AVT-AM formulation on A549 lung cancer cell lines. (a) Cell cycle analysis, (b) Apoptosis, and (c) Autophagy.

no significant changes in the proliferative effect at G0/G1 phase after 24 h, compared to the control cells. A significant increase was noticed in the G2/M−phase after the treatment for 24 h. This increased cell population to G2/M−phase was from 20.86 ± 1.97 % to 17.76 ± 1.17 %. When compared to control cells, this resulted in a significant cell cycle arrest in the G2/M phase. This result suggested that both cycle arrest at G2/M and apoptosis occurred simultaneously in A549 cells treated with AVT-AM. Additionally, the exposure of A549 cells to the formulation for 24 h resulted in a significant decrease in the sub-G1 cell population from 1.26 ± 0.08 % to 3.01 ± 0.87%. Remarkably, one of the anti-cancer action hallmarks is G2/M cell cycle arrest (Xu, Zhang, Qu, Jiang, & Li, 2011). Our results correlated with previous studies where cancer cells exposed to AVT-AM were arrested in G2/M (Fan et al., 2016; Fatehi Hassanabad & McBride, 2019; J. Lee et al., 2019; Tulbah, 2020; Zhang et al., 2019).

As a cancer treatment target, apoptosis or programmed cell death is considered (Abdelfadil et al., 2013; Hwang et al., 2012) Cells dying via necrosis versus apoptosis as shown in Fig. 7, B. The AVT-AM formula significantly induced early and late apoptosis (PI+ Annexin V−) by 1.22 and 1.28 folds, compared to control cells. The AVT-AM treatments resulted in a significant decrease in the survival rate of A549. It is demonstrated that about 0.23 ± 0.01 % and 0.87 ± 0.01 % of untreated A549 cells were in early and late apoptotic states, respectively, whereas AVT-AM treatment induced cell early and late apoptosis by about 0.28 ± 0.04 and 1.13 ± 0.12 %, respectively. As a result of these findings, A549 cells treated with AVT-AM experienced both apoptosis and cycle arrest at G2/M simultaneously. This finding was in alignment with the Lee et al. study (J. Lee et al., 2019). Additionally, significantly decreased necrotic phase (PI+ Annexin V−) percentages were found in proportion to the AVT-AM treatments (0.40 %), compared to the control cell (0.96 %), as shown in Fig (7, C). This could be because statins can promote cell death through one of two mechanisms: necrosis and apoptosis in several cell lines (Jafari, Rezaei, Kalantari, & Hashemitabar, 2013). Apoptosis is increased in cancer cells with intact apoptotic signalling pathways when autophagy is decreased (Ben Sahra et al., 2010). In A549 cells, the treatment with AVT-AM significantly inhibits autophagic cell death from 4,606,986 to 4,332,420, compared to control untreated cells (Fig. 7, C).

4. Conclusion

This study examined the impact of mannitol addition as a binder to improve the inhalation deposition and efficiency of the Atorvastatin Dry Powder formulation. AVT (0.2 % w/w) was successfully incorporated into a 99.8 % w/w of mannitol and spray dried to produce the AVT-AM microparticles formula. For inhalation therapy, the formula's particle size and aerosol performance met the criteria. Additionally, it was shown that AVT-AM formula is safe and nontoxic on A549. Compared to the free AVT, the cellular uptake of the AVT-AM formula in A549 cells was enhanced. Furthermore, the AVT-AM formula treatment induced apoptosis and caused G2/M arrest. Finally, these findings indicate that spray-dried mannitol microparticles could be a good candidate for delivering drugs for lung cancer treatment.

Funding

The authors would like to thank the Deanship of Scientific Research at Umm Al-Qura University for supporting this work by Grant Code 19-MED-1-02-0005.

Declaration of Competing Interest

The authors declare that they have no known competing financial interests or personal relationships that could have appeared to influence the work reported in this paper.

Acknowledgment

The authors would like to thank the Deanship of Scientific Research at Umm Al-Qura University for the Grant.

References

Abd-Elbary, A., El-Laithy, H., Tadros, M., 2008. Sucrose stearate-based proniosome-derived niosomes for the nebulisable delivery of cromolyn sodium. Int. J. Pharm. 357 (1–2), 189–198. https://doi.org/10.1016/j.ijpharm.2008.01.056.

Abdelfadil, E., Cheng, Y.-H., Bau, D.-T., Ting, W.-J., Chen, L.-M., Hsu, H.-H., Lin, Y.-M., Chen, R.-J., Tsai, F.-J., Tsai, C.-H., Huang, C.-Y., 2013. Thymoquinone induces apoptosis in oral cancer cells through p38β inhibition. Am. J. Chinese Med. 41 (03), 683–696.

Allam, R.M., Al-Abd, A.M., Khedr, A., Sharaf, O.A., Nofal, S.M., Khalifa, A.E., Mosli, H. A., Abdel-Naim, A.B., 2018. Fingolimod interrupts the cross talk between estrogen metabolism and sphingolipid metabolism within prostate cancer cells. Toxicol. Lett. 291, 77–85. https://doi.org/10.1016/j.toxlet.2018.04.008.

Bayón, R., Rojas, E., 2019. Development of a new methodology for validating thermal storage media: Application to phase change materials. Int. J. Energy Res. 43 (12), 6521–6541. https://doi.org/10.1002/er.v43.1210.1002/er.4589.

Ben Sahra, I., Laurent, K., Giuliano, S., Larbret, F., Ponzio, G., Gounon, P., Le Marchand-Brustel, Y., Giorgetti-Peraldi, S., Cormont, M., Bertolotto, C., Deckert, M., Auberger, P., Tanti, J.-F., Bost, F., 2010. Targeting cancer cell metabolism: the combination of metformin and 2-deoxyglucose induces p53-dependent apoptosis in prostate cancer cells. Cancer Res. 70 (6), 2465–2475. https://doi.org/10.1158/0008-5472.CAN-09-2782.

Byrne, A.J., Mathie, S.A., Gregory, L.G., Lloyd, C.M., 2015. Pulmonary macrophages: key players in the innate defence of the airways. Thorax 70 (12), 1189–1196.

Dixit, M., Kini, A., Kulkarni, P., 2010. Preparation and characterization of microparticles of piroxicam by spray drying and spray chilling methods. Res. Pharm. Sci. 5 (2), 89.

Dockery, D.W., Pope, C.A., Xu, X., Spengler, J.D., Ware, J.H., Fay, M.E., Ferris, B.G., Speizer, F.E., 1993. An association between air pollution and mortality in six US cities. N. Engl. J. Med. 329 (24), 1753–1759.

Dockery, D.W., Schwartz, J., Spengler, J.D., 1992. Air pollution and daily mortality: associations with particulates and acid aerosols. Environ. Res. 59 (2), 362–373.

Fan, Z., Jiang, H., Wang, Z., Qu, J., 2016. Atorvastatin partially inhibits the epithelial-mesenchymal transition in A549 cells induced by TGF-β1 by attenuating the upregulation of SphK1. Oncol. Rep. 36 (2), 1016–1022. https://doi.org/10.3892/or.2016.4897.

Fatehi Hassanabad, A., McBride, S.A., 2019. Statins as Potential Therapeutics for Lung Cancer. Am. J. Clin. Oncol. 42 (9), 732–736.

Fekry, M.I., Ezzat, S.M., Salama, M.M., Alshehri, O.Y., Al-Abd, A.M., 2019. Bioactive glycoalkaloides isolated from Solanum melongena fruit peels with potential anticancer properties against hepatocellular carcinoma cells. Scientific reports 9 (1), 1–11.

Ferdynand, M.S., Nokhodchi, A., 2020. Co-spraying of carriers (mannitol-lactose) as a method to improve aerosolization performance of salbutamol sulfate dry powder inhaler. Drug Delivery Translational Res. 10 (5), 1418–1427. https://doi.org/10.1007/s13346-020-00707-6.

Foster, K.A., Oster, C.G., Mayer, M.M., Avery, M.L., Audus, K.L., 1998. Characterization of the A549 cell line as a type II pulmonary epithelial cell model for drug metabolism. Exp. Cell Res. 243 (2), 359–366.

Gamal, A., Saeed, H., Sayed, O.M., Kharshoum, R.M., Salem, H.F., 2020. Proniosomal microcarriers: impact of constituents on the physicochemical properties of proniosomes as a new approach to enhance inhalation efficiency of dry powder inhalers. AAPS PharmSciTech 21, 1–12. https://doi.org/10.1208/s12249-020-01705-0.

Guntner, A.S., Doppler, C., Wechselberger, C., Bernhard, D., Buchberger, W., 2020. HPLC-MS/MS Shows That the Cellular Uptake of All-Trans-Retinoic Acid under Hypoxia Is Downregulated by the Novel Active Agent 5-Methoxyleoligin. Cells 9 (9), 2048.

Gupta, R., Vanbever, R., Mintzes, J., Nice, J., Chen, D., Batycky, R., Edwards, D., 2000. Physical characterization of large porous particles for inhalation. Pharm. Res. 17 (11), 1437–1438.

Hwang, J.-M., Ting, W.-J., Wu, H.-C., Chen, Y.-J., Tsai, F.-J., Chen, P.-Y., Liu, C.-Y., Chou, L.-C., Kuo, S.-C., Huang, C.-Y., 2012. KHC-4 anti-cancer effects on human PC3 prostate cancer cell line. Am. J. Chinese Med. 40 (05), 1063–1071.

Jafari, M., Rezaei, M., Kalantari, H., Hashemitabar, M., 2013. Determination of Cell Death Induced by Lovastatin on Human Colon Cell Line HT29 Using the Comet Assay. Jundishapur J. Nat. Pharm. Products 8 (4), 187–191. https://doi.org/10.17795/jjnpp-10951.

Kaialy, W., Martin, G.P., Larhrib, H., Ticehurst, M.D., Kolosionek, E., Nokhodchi, A., 2012a. The influence of physical properties and morphology of crystallised

lactose on delivery of salbutamol sulphate from dry powder inhalers. Colloids Surf., B 89, 29–39.
Kaialy, W., Ticehurst, M., Nokhodchi, A., 2012b. Dry powder inhalers: mechanistic evaluation of lactose formulations containing salbutamol sulphate. Int. J. Pharm. 423 (2), 184–194. https://doi.org/10.1016/j.ijpharm.2011.12.018.
Khurana, V., Bejjanki, H.R., Caldito, G., Owens, M.W., 2007. Statins reduce the risk of lung cancer in humans: a large case-control study of US veterans. Chest 131 (5), 1282–1288. https://doi.org/10.1378/chest.06-0931.
Kuh, H.J., Nakagawa, S.I., Usuda, J., Yamaoka, K., Saijo, N., Nishio, K., 2000. A computational model for quantitative analysis of cell cycle arrest and its contribution to overall growth inhibition by anticancer agents. Jpn J. Cancer Res. 91 (12), 1303–1313.
Lee, J., Jung, J.H., Hwang, J., Park, J.E., Kim, J.-H., Park, W.Y., Suh, J.Y., Kim, S.-H., 2019. CNOT2 is critically involved in atorvastatin induced apoptotic and autophagic cell death in non-small cell lung cancers. Cancers 11 (10), 1470. https://doi.org/10.3390/cancers11101470.
Lee, W.-H., Loo, C.-Y., Ghadiri, M., Leong, C.-R., Young, P.M., Traini, D., 2018. The potential to treat lung cancer via inhalation of repurposed drugs. Adv. Drug Deliv. Rev. 133, 107–130.
Lee, W.-H., Loo, C.-Y., Ong, H.-X., Traini, D., Young, P.M., Rohanizadeh, R., 2016. Synthesis and characterization of inhalable flavonoid nanoparticle for lung cancer cell targeting. J. Biomed. Nanotechnol. 12 (2), 371–386.
Lee, W.-H., Loo, C.-Y., Traini, D., Young, P.M., 2021. Development and evaluation of paclitaxel and curcumin dry powder for inhalation lung cancer treatment. Pharmaceutics 13 (1), 9.
Lieber, M., Todaro, G., Smith, B., Szakal, A., Nelson-Rees, W., 1976. A continuous tumor-cell line from a human lung carcinoma with properties of type II alveolar epithelial cells. Int J Cancer 17 (1), 62–70. https://doi.org/10.1002/ijc.2910170110.
Lin, J.J., Ezer, N., Sigel, K., Mhango, G., Wisnivesky, J.P., 2016. The effect of statins on survival in patients with stage IV lung cancer. Lung Cancer 99, 137–142. https://doi.org/10.1016/j.lungcan.2016.07.006.
Lohmann-Matthes, M., Steinmuller, C., Franke-Ullmann, G., 1994. Pulmonary macrophages. Eur. Respir. J. 7 (9), 1678–1689.
Marin, L., Traini, D., Bebawy, M., Colombo, P., Buttini, F., Haghi, M., Ong, H.X., Young, P., 2013. Multiple dosing of simvastatin inhibits airway mucus production of epithelial cells: implications in the treatment of chronic obstructive airway pathologies. Eur. J. Pharm. Biopharm. 84 (3), 566–572.
Mohning, M.P., Thomas, S.M., Barthel, L., Mould, K.J., McCubbrey, A.L., Frasch, S.C., Bratton, D.L., Henson, P.M., Janssen, W.J., 2018. Phagocytosis of microparticles by alveolar macrophages during acute lung injury requires MerTK. Am. J. Physiol.-Lung Cellular Mol. Physiol. 314 (1), L69–L82.
Mörbt, N., Tomm, J., Feltens, R., Mögel, I., Kalkhof, S., Murugesan, K., Wirth, H., Vogt, C., Binder, H., Lehmann, I., von Bergen, M., 2011. Chlorinated benzenes cause concomitantly oxidative stress and induction of apoptotic markers in lung epithelial cells (A549) at nonacute toxic concentrations. J. Proteome Res. 10 (2), 363–378.
Mustafa, M., Azizi, AR.J., IIIzam, E.L., Nazirah, A., Sharifa, S., Abbas, S.A., 2016. Lung cancer: risk factors, management, and prognosis. IOSR J. Dental Med. Sci. 15 (10), 94–101. https://doi.org/10.9790/0853-15100494101.
Newman, S.P., 1985. Aerosol deposition considerations in inhalation therapy. Chest 88 (2), 152S–160S.
Ong, H.X., Traini, D., Ballerin, G., Morgan, L., Buddle, L., Scalia, S., Young, P.M., 2014. Combined inhaled salbutamol and mannitol therapy for mucus hyper-secretion in pulmonary diseases. AAPS J. 16 (2), 269–280.
Peng, T., Lin, S., Niu, B., Wang, X., Huang, Y., Zhang, X., Li, G.e., Pan, X., Wu, C., 2016. Influence of physical properties of carrier on the performance of dry powder inhalers. Acta Pharmaceutica sinica B 6 (4), 308–318.
Pharmacopeia, U. (2015). Inhalation and Nasal Drug Products: Aerosols, Sprays, and Powders— Performance Quality. In: *United States Pharmacopeia, USP 38–NF 33nd Supplement* (33 ed., Vol. 4/a, pp. 388-413): US Pharmacopeial Convention: Rockville, MD.
Plumley, C., Gorman, E.M., El-Gendy, N., Bybee, C.R., Munson, E.J., Berkland, C., 2009. Nifedipine nanoparticle agglomeration as a dry powder aerosol formulation strategy. Int. J. Pharm. 369 (1-2), 136–143.
Pope, C.A., Thun, M.J., Namboodiri, M.M., Dockery, D.W., Evans, J.S., Speizer, F.E., Heath, C.W., 1995. Particulate air pollution as a predictor of mortality in a prospective study of US adults. Am. J. Respir. Crit. Care Med. 151 (3), 669–674.
Pucci, B., Kasten, M., Giordano, A., 2000. Cell cycle and apoptosis. Neoplasia 2 (4), 291–299.
Saeed, H., Salem, H.F., Rabea, H., Abdelrahim, M.E.A., 2019. Effect of human error, inhalation flow, and inhalation volume on dose delivery from Ellipta® dry-powder inhaler. J. Pharmaceutical Innovation 14 (3), 239–244.
Salem, H., Abdelrahim, M., Eid, K.A., Sharaf, M., 2011. Nanosized rods agglomerates as a new approach for formulation of a dry powder inhaler. Int. J. Nanomed. 6, 311.
Schneider, D.J., Speth, J.M., Penke, L.R., Wettlaufer, S.H., Swanson, J.A., Peters-Golden, M., 2017. Mechanisms and modulation of microvesicle uptake in a model of alveolar cell communication. J. Biol. Chem. 292 (51), 20897–20910.
Schwartz, J., Dockery, D.W., 1992. Increased mortality in Philadelphia associated with daily air pollution concentrations. Am. Rev. Respiratory Dis. 145 (3), 600–604.
Shahraeini, S.S., Akbari, J., Saeedi, M., Morteza-Semnani, K., Abootorabi, S., Dehghanpoor, M., Rostamkalaei, S.S., Nokhodchi, A., 2020. Atorvastatin Solid Lipid Nanoparticles as a Promising Approach for Dermal Delivery and an Anti-inflammatory Agent. AAPS PharmSciTech 21 (7). https://doi.org/10.1208/s12249-020-01807-9.
Singh, S., Changotra, H., 2019. FDFT1 Variant rs2645429 and Cancer Susceptibility in Himachal Population.
Stanisz, B., Kania, L., 2006. Validation of HPLC method for determination of atorvastatin in tablets and for monitoring stability in solid phase. Acta Pol. Pharm. 63 (6), 471–476.
Stearns, R.C., Paulauskis, J.D., Godleski, J.J., 2001. Endocytosis of ultrafine particles by A549 cells. Am. J. Respir Cell Mol. Biol. 24 (2), 108–115. https://doi.org/10.1165/ajrcmb.24.2.4081.
Steckel, H., Bolzen, N., 2004. Alternative sugars as potential carriers for dry powder inhalations. Int. J. Pharm. 270 (1-2), 297–306.
Tee, S.K., Marriott, C., Zeng, X.M., Martin, G.P., 2000. The use of different sugars as fine and coarse carriers for aerosolised salbutamol sulphate. Int. J. Pharm. 208 (1-2), 111–123.
Tulbah, A.S., 2020. The potential of Atorvastatin for chronic lung diseases therapy. Saudi Pharmaceutical J.: SPJ 28 (11), 1353–1363.
Tulbah, A.S., Ong, H.X., Morgan, L., Colombo, P., Young, P.M., Traini, D., 2015. Dry powder formulation of simvastatin. Expert Opinion Drug Delivery 12 (6), 857–868. https://doi.org/10.1517/17425247.2015.963054.
Tulbah, A.S., Pisano, E., Landh, E., Scalia, S., Young, P.M., Traini, D., Ong, H.X., 2019. Simvastatin nanoparticles reduce inflammation in LPS-stimulated alveolar macrophages. J. Pharm. Sci. 108 (12), 3890–3897. https://doi.org/10.1016/j.xphs.2019.08.029.
Vanbever, R., Mintzes, J.D., Wang, J., Nice, J., Chen, D., Batycky, R., Edwards, D.A., 1999. Formulation and physical characterization of large porous particles for inhalation. Pharm Res 16 (11), 1735–1742.
Xia, D.-K., Hu, Z.-G., Tian, Y.-F., Zeng, F.-J., 2019. Statin use and prognosis of lung cancer: a systematic review and meta-analysis of observational studies and randomized controlled trials. Drug Des., Development Therapy 13, 405.
Xu, X., Zhang, Y., Qu, D., Jiang, T., Li, S., 2011. Osthole induces G2/M arrest and apoptosis in lung cancer A549 cells by modulating PI3K/Akt pathway. J. Exp. Clin. Cancer Res. 30 (1), 1–7.
Young, P.M., Traini, D., Coates, M., Chan, H.-K., 2007. Recent advances in understanding the influence of composite-formulation properties on the performance of dry powder inhalers. Physica B 394 (2), 315–319.
Zhang, L., Chen, T., Dou, Y., Zhang, S., Liu, H., Khishignyam, T., Li, X., Zuo, D., Zhang, Z., Jin, M., Wang, R., Qiu, Y., Zhong, YuXu, Kong, D., 2019. Atorvastatin exerts antileukemia activity via inhibiting mevalonate-YAP Axis in K562 and HL60 Cells. Front. Oncol. 9. https://doi.org/10.3389/fonc.2019.01032.
Zijlstra, G.S., Rijkeboer, M., van Drooge, D.J., Sutter, M., Jiskoot, W., van de Weert, M., Hinrichs, W.L.J., Frijlink, H.W., 2007. Characterization of a cyclosporine solid dispersion for inhalation. AAPS J. 9 (2), E190–E199.